2024 7th International Conference on Soft Robotics (RoboSoft)
San Diego, CA, USA. April 14-17, 2024

Interaction Behaviors of a Vine Robot in a Pipe T-Junction

Lily Behnke[1], Brian H. Do[1], Sophia Eristoff[1], and Rebecca Kramer-Bottiglio[1]

***Abstract*— Continuous advances in soft robotic technologies have promoted the feasibility of exploration of complex environments and terrains. One prominent example is the class of tip-everting "vine" robots, which have enabled a new set of real-world applications. Vine robots navigate their environment through growth and have recently been used in practice for in-pipe inspection, maintenance, and exploration. While locomotion through these directed cylindrical systems is simplified by a vine robot's growth, there are challenges with navigation. In complex pipe networks with many junctions, one question is how a vine can navigate around its own body during exploration. For example, a vine may navigate a pipe network that forces the robot to traverse a section of a pipe it already traversed in the opposite direction. This work presents an experimental approach to investigating and characterizing the interaction of a vine with its own body inside of a pipe T-junction. The results of this work provide initial design recommendations for facilitating the successful navigation of a vine robot in a T-junction.**

I. INTRODUCTION

Exploring confined environments and complex terrain is a major goal in robotics, but navigation in confined, complex, or viscous spaces is difficult for traditional gait-based systems [1]. While soft robots aim to accomplish tasks such as search and rescue, ecological monitoring, medical intervention, and industrial maintenance, challenges still exist for navigation of the aforementioned environments [2]–[4]. As such, a class of soft robots known as vine robots that locomote through growth has been leveraged to address the limitations of other robots in exploration [5].

One application that necessitates such exploration is in-pipe inspection and maintenance [6]. Pipes and pipelike structures are ubiquitous in modern society, ranging from oil and water pipelines to air ducts. Research into in-pipe locomoting robots extends back decades, but navigating through variable diameter pipes and complex pipe networks involving T-junctions remains challenging [6].

Vine robots are especially well-suited for such applications. One of the most applied use cases for vine robots has been the exploration of networks such as electrical conduits, tunnels, and pipes [7]–[10]. However, since vine robots move through the growth of their own bodies, tunnel or pipe environments with loops or intersecting branches, a vine robot may have to navigate around its own body for continued locomotion. While a key advantage of soft robots is their ability to easily interact with their environments and leverage these interactions, previous work has only characterized vine robot interactions with rigid environments and obstacles [11]–[13]. Vine robot interactions with compliant or compliance-matched objects, such as its own body, have been much less studied.

[1]School of Engineering and Applied Sciences, Yale University, New Haven, CT, USA email:{lily.behnke, brian.do, sophia.eristoff, rebecca.kramer}@yale.edu

L.B. was supported by the National Science Foundation Graduate Research Fellowship (DGE-2139841). B.H.D. was supported by the National Science Foundation under grant no. IIS-1955225. S.E. was supported by the NASA NSTGRO fellowship (80NSSC21K1269).

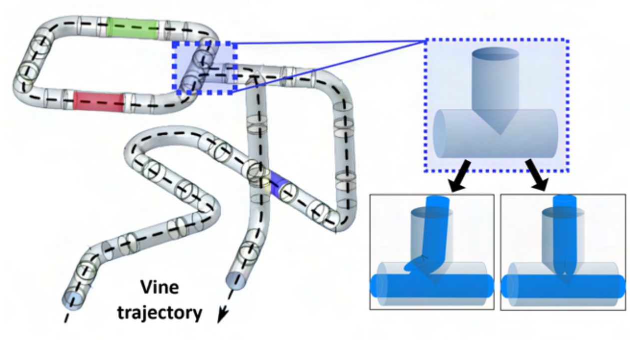

Fig. 1. A pipe network with a magnified inset of the T-junction along a vine robot trajectory. The two schematics indicate two potential outcomes of the vine robot coming into contact with its own body: one that allows continued locomotion and one that stalls locomotion.

To exemplify the relevance of pipe navigation as a grand challenge in soft robotics, the 2023 IEEE International Conference on Soft Robotics (RoboSoft) held a competition on "in-pipe locomotion," featuring a mazelike pipe network for robots to autonomously navigate [14]. This challenge mimicked a real-world scenario where the task completion required navigating through a T-junction as shown in Fig. 1. A vine robot was indeed used in the competition and won third place, although failed to navigate through the T-junction to complete the course. This prior Robosoft competition result further motivated the work herein.

In this work, we characterize passive vine robot self-interaction behavior inside a pipe T-junction. We also explore the capabilities of vine robots to locomote through a pipe and environments with self-constrained boundaries. The results of this study aim to provide insight into basic design parameters that promote successful continued locomotion for vine robots that intersect their own bodies inside pipe T-junctions.

II. BEHAVIOR CHARACTERIZATION

A. Experimental Setup

To characterize the behavior of a vine robot in a pipe T-junction, an experimental setup consisting of an inlet, loop, and T-junction was constructed from clear 6.35 cm diameter pipes (Jumpanny). Vine robots were fabricated from 1.3 oz silicone-impregnated ribstop nylon (Seattle Fabrics) and were each 150 cm in length with varying diameters. A Nikon

2024 IEEE 7th International Conference on Soft Robotics (RoboSoft) | 979-8-3503-8181-8/24/$31.00 ©2024 IEEE | DOI: 10.1109/ROBOSOFT60065.2024.10522034

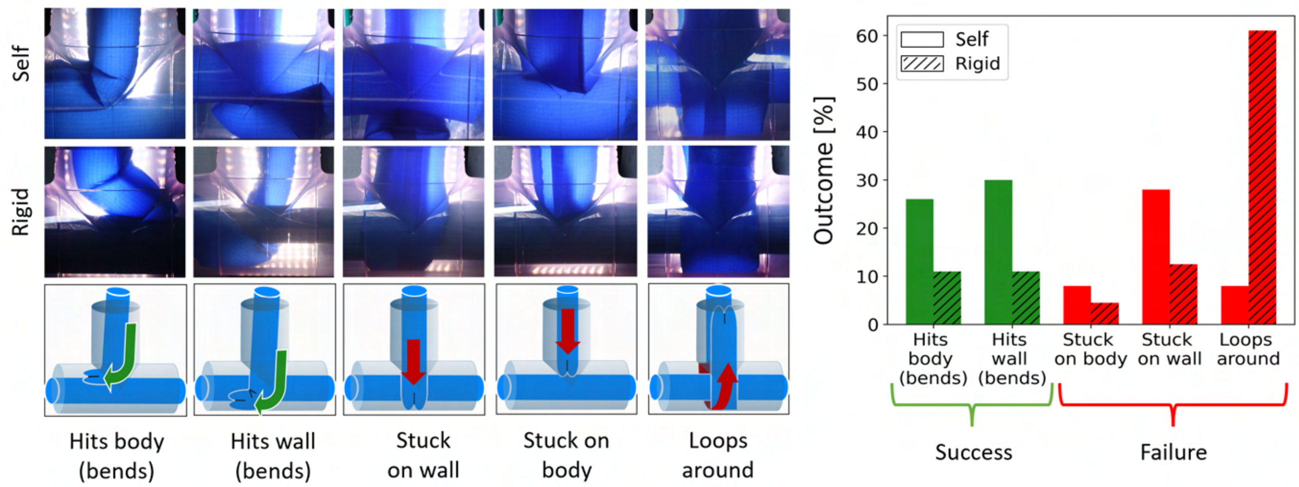

Fig. 2. Still images of the behaviors demonstrated by a $D_r/D_p = 0.68$ vine robot in a pipe T-junction for self and rigid rod collisions with accompanying schematic visual representations. Bar chart showing the outcome percentage of each behavior across both collision types (rigid and self) for all vine robot diameters and operating pressures. The red and green coloring separates the behaviors into whether locomotion continued successfully or failed.

camera was positioned above the T-junction to record the vine interaction and trajectory. For each trial, the vine robot was placed at the inlet and pressurized to begin tip eversion. The robot traversed through the base of the T-junction before looping around to the top of the T-junction via three pipe elbows, ultimately directing the vine to contact itself.

A similar setup was made using a rigid rod as an obstacle in the T-junction. This rigid interaction was used as a control since the interactions of vine robots with rigid structures are more defined in literature [11]–[13]. For each vine tested, a PLA rod of the same diameter was placed in the T-junction base during testing. The vine robots were pressurized from an inlet point after the T-junction base and then passed through three pipe elbows to approach the T-junction and interact with the rigid rod.

Each self-interaction and interaction with a rigid rod was carried out at five different pressures (50, 70, 90, 110, and 130 kPa) and four vine diameters (2.25, 3.25, 4.25, and 5.25 cm). Diameter and pressure were investigated because they are two universally controllable design parameters for vine robots. For each interaction at a given diameter and pressure, 10 interactions were recorded; in total, there were 200 trials for both the rigid and self characterizations. Figure 2 shows segmented still images of the resulting vine robot behaviors and success vs. failure characterizations with respect to continued locomotion through the T-junction.

B. Characterization

Figure 2 shows the characterized behaviors and frequency for both interaction types, also categorizing the behaviors as a success or failure. Success was defined as the vine robot continuing locomotion to the completion of its length, left or right, after colliding with the body in the junction, and any other outcome was defined as a failure. The images to the left of the plot show stills of each behavior for both self and rigid interactions and schematics of the behavior. During locomotion inside the T-junction, the vine robot exhibited one of five behaviors: When successful, the vine either 1) hit the body and then bent left or right to continue locomotion or 2) moved past the body and hit the wall to then bend left or right. When unsuccessful, the vine either 3) got stuck on the body it collided with, 4) moved past the body and got stuck on the wall, or 5) looped around the body to continue locomotion in the direction of approach.

It was hypothesized that a vine colliding with its own body would pose a treacherous obstacle due to the matched compliance of the bodies. However, it can be observed in Fig. 2 that a vine colliding with its own body showed greater success than a vine interacting with a rigid rod. In fact, self-interaction behavior demonstrates greater success than interaction with a rigid rod in both success categories. Furthermore, it was observed that failure due to the vine looping around the rigid rod was the most common outcome across all experiments; this is consistent with prior work on vine robot interactions with rigid barriers [11]. Generally, the outcomes in Fig. 2 demonstrate that contact with a compliance-matched body better facilitates T-junction navigation compared to with a rigid body.

III. SELF-CONTACT OUTCOMES

After observing that the self-contact of a vine robot facilitates successful T-junction navigation, we further investigated this behavior. We characterized each instance where the vine was observed hitting its own body, buckling, and then successfully continuing locomotion, which occurred in 53 out of the 200 tests conducted. We then performed motion tracking of the vine self-contact in post-processing (Tracker Inc.). The pose of the approaching vine tip to the stationary vine body was tracked throughout the buckling behavior, and the contact angle between the bodies was calculated. The initial time stamp for the analysis was when the vine robot first made contact with its own body, and the final time stamp was marked just after the vine robot buckled and the axial portion of the vine above the buckle point stabilized.

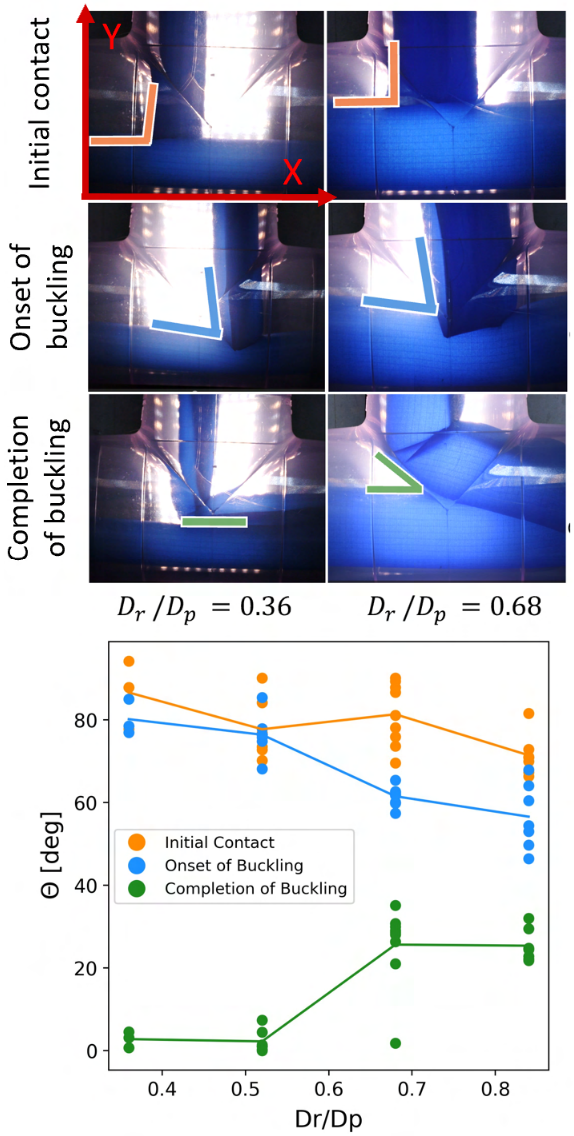

Fig. 3. *Top:* Still images showing contact angle during initial contact at the onset of buckling and at the completion of buckling for small and large diameter vine robots. *Bottom:* Graph of contact angles vs diameters. The scatter plot points represent the angle for each occurrence of the behavior for the respective vine diameter while the line represents the average.

Figure 3 shows the resulting progression of the contact angle throughout this self-intersection behavior as a function of vine diameter. The plot's x-axis represents the ratio D_r/D_p of the vine robot diameter D_r to the diameter of the pipe D_p. The three lines on the plot represent key events in this motion: initial contact, buckling onset, and completion of buckling; stills of these events are shown in Fig. 3.

The initial contact angle (orange) was similar for all vine robot diameters, ranging between 75° and 90°, indicating this initial contact angle may be required for self-intersection behavior. Furthermore, for small-diameter vines ($D_r/D_p =$ 0.36 and 0.52), only a marginal difference exists between the initial contact angle (orange) and the onset of buckling angle (blue). However, for larger diameter vines ($D_r/D_p = 0.68$ and 0.84), the average difference between the initial contact angle and the onset of buckling differs by about 15°. This suggests that repositioning is required by larger-diameter vines to achieve buckling during a self-interaction. Moreover, the angle at the completion of buckling also differs between small and large-diameter vines. As shown in the still images for the $D_r/D_p = 0.36$ vine, buckling occurs further in the positive y-direction from the contact point and causes the vine to buckle to 0 degrees relative to the stagnant part of the body parallel to the x-axis. This buckling behavior is reflected in the large difference between the onset and completion of buckling angles. However, for larger diameter vines, Fig. 3 shows that the difference between the onset of and completion of buckling is more narrow. This can be observed by the corresponding sequence of images for the $D_r/D_p = 0.68$ vine, where buckling occurs at the tip of the approaching body where the contact takes place.

IV. DESIGN PARAMETER INVESTIGATION

In this section, we analyze how three design parameters—diameter, pressure, and stiffness—affect successful vine robot traversal in a T-junction. We also relate results from empirical tests, summarized in Fig. 4, to interaction models.

A. Diameter

As shown in Fig. 3, vine robot diameter plays a critical role in the buckling progression of the robot. Since buckling is a vine robot's key mode of enabling locomotion when encountering a barrier, it was anticipated that vine-robot locomotion in a T-junction would be diameter-dependent. Figure 4 demonstrates this diameter dependency on the success mode and frequency in a T-junction as well as the relationship between compressive modulus and diameter. In Fig. 4 (a)-(e), the results from the self-interaction experiments are plotted as a function of D_r/D_p for the five pressures tested. The points in Fig. 4 (a)-(e) show the total success percentage of each diameter vine robot across the five tested internal pressures. The bars under each point represent the contribution of each successful behavior toward the total. The two behaviors categorized as successful navigation are illustrated by the schematics in Fig. 4 (f) and (g), respectively.

We observed that smaller diameter vine robots are more successful than larger diameters ones at navigating a T-junction. The smallest diameter vine robot ($D_r/D_p = 0.36$) was the most successful for 4 of the 5 operating pressures, as shown in Fig. 4 ((a)-(e)). This trend further extends to the second smallest vine robot diameter tested ($D_r/D_p = 0.52$) which was the second most successful diameter with all the pressures considered.

Smaller vine diameters are less likely to come into contact with their own bodies in the T-junction. From Greer et al. [11], when the tip of the vine robot is in contact with a rigid obstacle and free growth is possible, the robot tip will move parallel to the obstacle surface, pivoting about the last previous point of contact. The reaction force from the obstacle will cause the vine robot to buckle about that pivot point, allowing the robot to move around that obstacle.

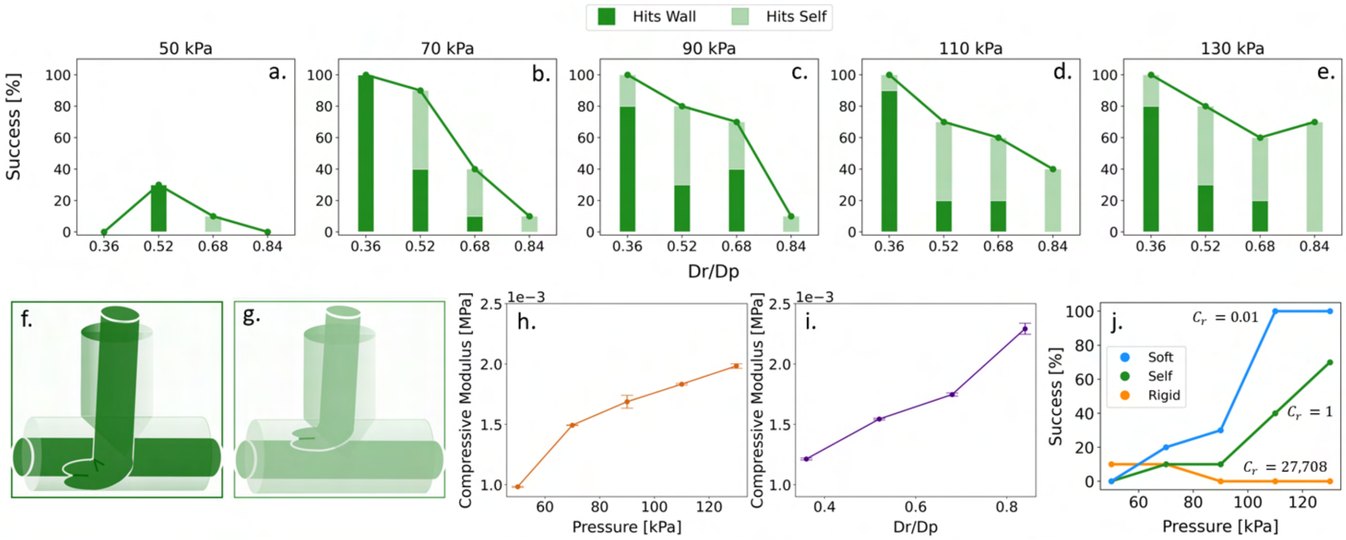

Fig. 4. a-e) Frequency of successful navigation of a pipe T-junction for a vine robot as a function of pressure and diameter. f-g) Schematics of successful navigation modes corresponding to the bar chart compositions in a-e. h) Compressive modulus of a vine robot of constant diameter ($D_r/D_p = 0.68$) as a function of pressure. i) Compressive modulus of a vine robot of constant pressure (90 kPa) as a function of diameter. j) Success frequency of three case studies where a $D_r/D_p = 0.84$ vine approaches itself (compliance-matching; green), a rigid rod (orange), and a soft foam cylinder (blue) in a pipe T-junction.

For smaller diameter vines, this obstacle interaction dominates as the vine either misses its body and simply slides along the inside of the T-junction wall or slides around its body before proceeding to the wall. The tip of the robot will slide as it pivots about the top of the T junction until it undergoes transverse buckling and completes the 90° turn to the other branches of the pipe network.

However, this trend does not extend to larger vine diameters, where the primary success mode was through self-contact. The data in Fig. 4 (a)-(e) show each success mode's frequency. Besides the smallest vine robot diameter ($D_r/D_p = 0.36$), successful navigation due to self-contacts was more frequent than successful navigation from a wall contact because large diameter vines have less free space within the T-junction and thus must interact themselves.

B. Pressure

We also investigated the effect of the vine robot's internal pressure. Each plot in Fig. 4 (a)-(e) also presents the relationship between pressure and navigation success. At an operation pressure of 50 kPa, no vine robot was notably more successful in navigating the pipe T-junction, indicating that this pressure did not produce the critical force for the vine robot to consistently buckle. However, at 70 kPa (Fig. 4 (b)), overall success increases for all tested diameters. Aside from 50 kPa, the total success rates of smaller diameter vine robots were consistent. However, at larger vine robot diameters there is an increase in vine robot success as a function of pressure. Specifically, for $D_r/D_p = 0.84$, there is a steady increase in success due to self-contact from 50-130 kPa.

The vine robot can be modeled as an inflated beam. When the vine robot operates in a constrained environment, such as a pipe network, it navigates by reconfiguring its body. This reconfiguration occurs through buckling caused by the forces the vine robot applies to its environment. In the T-junction, when the robot hits its body head-on, it must undergo axial buckling before continuing to traverse the pipe network. From Fichter [15], the critical force for axial buckling is:

$$F_{cr} = \frac{EI\frac{\pi^2}{L^2}\left(PA + \frac{\pi}{2}GD_r t\right)}{EI\frac{\pi^2}{L^2} + PA + \frac{\pi}{2}GD_r t} \tag{1}$$

where E, G, and t are Young's modulus, shear modulus, and thickness of the wall material, respectively; I is the beam second moment of area; P is the internal pressure; A is the cross-sectional area; and L is the length of the robot body.

When interacting with its environment, the vine robot is subject to a reaction force $F = PA$ resulting from its attempted growth. If $F > F_{cr}$, the robot will buckle. If the force is not high enough to cause immediate buckling, the robot may end up getting stuck on its body or slipping around its body and failing to buckle to successfully navigate the T-junction. This explains why increasing P promotes buckling, as it can increase F so that $F > F_{cr}$.

Equation 1 can be rewritten to explicitly solve for the critical pressure P_{cr} for buckling. Substituting $F_{cr} = P_{cr}A$ into Eq. 1 and solving for P_{cr}, we find that increasing D_r increases the required P_{cr} and F_{cr} for buckling.

One key difference between this work and past work is that the vine robot interacts with a *compliant* obstacle—its own body. When the vine robot hits its body, both the tip and the body deform. This deformation plays a key role in keeping the robot tip perpendicular to the body until wrinkling propagates around the circumference of the body, enabling self-buckling and successful traversal of the T-junction. At larger diameters, the vine robot always hits its own body, and this compliant interaction is key in successful traversal. Modeling this compliant interaction is complex and will be addressed in future work.

C. Stiffness

Prior work has shown that variable stiffness can facilitate vine robot shape change [16], [17]. Our observation of increased navigation success with increased pressure for large diameter vines prompted a deeper investigation into the relationship between stiffness and navigation success.

1) Compressive Modulus: We tested how the vine robot's compressive modulus varies with diameter and pressure. We conducted compression tests on representative inflated beams for a constant pressure (90 kPa) with varied diameter and for a constant diameter ($D_r/D_p = 0.68$) with varied pressure. Using a universal testing machine (Instron 3345), samples were loaded transversely on a flat plate and compressed to 50% displacement at a rate of 5 mm/s. The resulting stress vs. strain curves were obtained, and their slopes were used to obtain the compressive modulus. Each sample was tested 5 times at each condition. Figure 4 (h)-(i) show the results.

Increasing compressive modulus increases navigation success. Figure 4 (h) presents the relationship of inflated beam compressive modulus with pressure. The inflated beam compressive modulus increases as a function of input pressure for the tested range (50-130 kPa).

Figure 4 (i) presents the relationship between compressive modulus and inflated beam diameter. Inflated beam diameter is reported as a ratio with respect to pipe diameter for consistency. The results show that inflated beam compressive modulus increases as a function of diameter. For larger diameter vines, increased pressures resulted in a greater propensity for successful T-junction navigation (Fig. 4 (a)-(e)). Larger diameters guarantee vine contact in a T-junction, resulting in a dependence on this material interaction.

2) Compliance Mismatch: When changing pressure alone, the stiffness of the entire vine increases together; the tip and body compliance are matched. To further investigate the effect of stiffness on vine interactions, we also looked at cases of large compliance mismatch between the vine tip and the body it interacted with. We conducted three case studies for a constant D_r/D_p (0.84): a vine colliding with 1) its own body, 2) a rigid PLA body, and 3) a soft foam body; tests were performed for a constant diameter over a range of pressures. The ratio between the compressive modulus of the stagnant body and the approaching body was reported as a compliance ratio as denoted by C_r in Fig. 4 (j). Case 2 and 3 act as bounding controls for compliance mismatched collisions, while case 1 reflects the work observed thus far. The same experimental procedure outlined in Sec. II was used for each case, and the results are shown in Fig. 4 (j).

Figure 4 (j) shows that all cases at low pressures ($<$90 kPa) have relatively similar success rates. However, at higher pressures ($>$90 kPa), the success rates diverge. For case 2, where the robot encounters a rigid rod, there is a low success rate, which follows the observations shown in Fig. 2. For case 1 an increase in pressure (and therefore compressive modulus) facilitates success. Finally, case 3, where the more rigid vine robot encounters the soft foam cylinder, shows the highest success rate.

Figure 2 (j) implies that for matched compliance interactions, successful buckling and continued locomotion are facilitated by increased stiffness. However, for mismatched compliance vine interactions, collisions with soft bodies produces greater success for continued trajectory compared to rigid bodies. Very rigid objects act as rigid obstacles which often deflect the robot around them, leading the vine robot to loop around rather than self-buckle. Meanwhile, very compliant objects are compressed by the vine robot and conform to the T-junction interior walls or are simply pushed out of the way. Afterwards, the typical vine interactions in constrained environments occur and the vine tip slides along the surface until it buckles and exits the T-junction.

V. GUIDELINES AND DEMONSTRATION

1) Design Parameter Guidelines: In pipe exploration, T-junctions are a complex boundary condition that will be encountered by vine robots. As such, extensive characterization was performed to identify the passive behavior of vine robots in a T-junction as a function of diameter and operation pressure. It is understood that these variables play an important role in dictating the material and geometric state of a vine robot. Through analysis of the observed outcomes, we drew insights into which parameters would aid in facilitating a vine robot's successful navigation through a T-junction.

Throughout this study, we observed that small diameter vines have the greatest success overall. By avoiding self-contact, small diameter vines leverage rigid body interactions where they hit the wall and then bend for successful navigation. In contrast, larger diameter vines inherently guarantee self-contact, and therefore are unable to isolate a compliance mismatch. These larger diameter vines demonstrated more successful navigation with increased operation pressure, which corresponds to an increase in compressive modulus. Finally, we showed that the compliance mismatch in which the vine robot contacts a much softer foam body also increased navigation success in a pipe T-junction.

2) Demonstrations: We can leverage the aforementioned guidelines to enable vine robot traversal of network junctions. Three demonstrations were performed to show how changing design parameters can promote the ability of a vine robot to successfully navigate through a T-junction. Figure 5 shows still images from a demonstration video with methods for facilitating T-junction navigation. The top left shows a failed condition where the vine robot becomes stuck on itself. We showcase three modifications that can facilitate successful navigation. In the first scenario (bottom left), a variable diameter vine was created. The vine was designed so that sections inside the T-junction had reduced diameter. By reducing the diameter, the vine undergoes a traditional wall interaction and does not pose as a barrier to itself, resulting in successful navigation. In the second scenario (top right), a varied stiffness patch was added to the approaching part of a vine robot to induce a compliance mismatch in which the approaching body is stiffer than the stagnant body resulting in a high frequency of success.

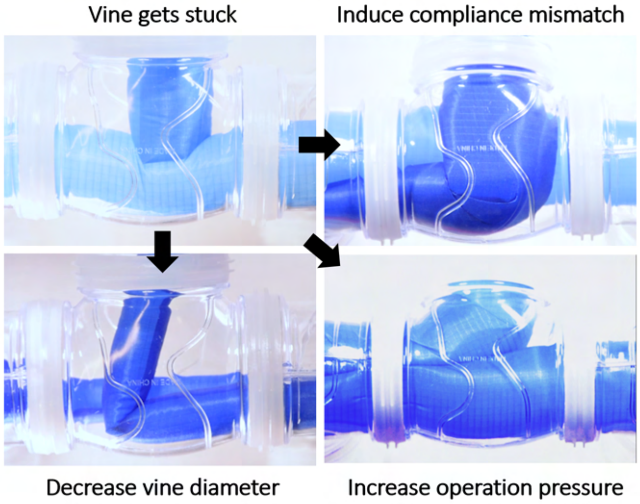

Fig. 5. Still images from a demonstration detailing three design choices that facilitate the successful navigation of a vine robot in a pipe T-junction.

Finally, in the third scenario (bottom right), the operation pressure of the body was increased; for large values of D_r/D_p, successful navigation of a T-junction when a vine interacts with itself increases with operation pressure. All of these design parameter changes facilitate successful T-junction navigation.

VI. CONCLUSION

In this work, we characterized the interaction behaviors of and provided design guidelines for successful vine robot navigation in pipe junctions. The behaviors of vine self-interaction and rigid rod interactions were investigated and compared. The self-contact behavior, which resulted in a vine robot hitting itself, buckling, and continuing locomotion through a T-junction, was evaluated. The resulting success rate of vine robot self-contacts was then investigated with respect to diameter and pressure. Geometrical properties dominate vine robot success for small diameters where contact is not guaranteed for a vine robot with itself. In contrast, at large diameters where vine robot contact is guaranteed within the T-junction, material properties dominate the interaction behaviors. Furthermore, for larger diameter cases where contact is guaranteed, it was observed that the frequency of successful navigation from self-contact is increased by vine stiffness. Finally, we demonstrated how insights from observations can be implemented in vine robot designs—such as using a varied diameter, increased operating pressure, or compliance mismatched vine robot—to facilitate successful navigation through a T-junction.

The results of this study have introduced a need for further investigation into the characterization of vine robot interactions with soft matter. Future work aims to introduce mechanical models to elaborate upon the experimental findings in the work, such as precisely modeling the interaction of the vine robot with compliant objects. Additionally, work remains to understand vine robot locomotion through a variety of complex applications systems such as in vivo, underground, and through various media. By altering the diameter and operation pressure of a vine robot, greater success for continued navigation within a pipe T-junction for exploration could be realized. We foresee this work having broader applications in the fields of pipe inspection and maintenance where optimizing self-interaction will be critical in the successful operation of vine robots, making them more accessible in real-world settings.

REFERENCES

[1] P. E. Glick, I. Adibnazari, D. Drotman, D. Ruffatto III, and M. T. Tolley, "Branching vine robots for unmapped environments," *Frontiers in Robotics and AI*, vol. 9, 2022.

[2] M. Khazanov, J. Jocque, and J. Rieffel, "Evolution of locomotion on a physical tensegrity robot," in *Artificial Life Conference Proceedings*, pp. 232–238, MIT Press, Cambridge, MA, USA, 2014.

[3] S. M. Youssef, M. Soliman, M. A. Saleh, M. A. Mousa, M. Elsamanty, and A. G. Radwan, "Underwater soft robotics: A review of bioinspiration in design, actuation, modeling, and control," *Micromachines*, vol. 13, no. 1, p. 110, 2022.

[4] M. Cianchetti, C. Laschi, A. Menciassi, and P. Dario, "Biomedical applications of soft robotics," *Nature Reviews Materials*, vol. 3, no. 6, pp. 143–153, 2018.

[5] E. W. Hawkes, L. H. Blumenschein, J. D. Greer, and A. M. Okamura, "A soft robot that navigates its environment through growth," *Science Robotics*, vol. 2, no. 8, p. eaan3028, 2017.

[6] J. T. Kahnamouei and M. Moallem, "A comprehensive review of in-pipe robots," *Ocean Engineering*, vol. 277, p. 114260, 2023.

[7] M. M. Coad, L. H. Blumenschein, S. Cutler, J. A. R. Zepeda, N. D. Naclerio, H. El-Hussieny, U. Mehmood, J.-H. Ryu, E. W. Hawkes, and A. M. Okamura, "Vine robots," *IEEE Robotics & Automation Magazine*, vol. 27, no. 3, pp. 120–132, 2019.

[8] L. H. Blumenschein, M. M. Coad, D. A. Haggerty, A. M. Okamura, and E. W. Hawkes, "Design, modeling, control, and application of everting vine robots," *Frontiers in Robotics and AI*, vol. 7, 2020.

[9] M. Wooten, C. Frazelle, I. D. Walker, A. Kapadia, and J. H. Lee, "Exploration and inspection with vine-inspired continuum robots," in *IEEE International Conference on Robotics and Automation*, pp. 5526–5533, IEEE, 2018.

[10] P. A. Der Maur, B. Djambazi, Y. Haberthür, P. Hörmann, A. Kübler, M. Lustenberger, S. Sigrist, O. Vigen, J. Förster, F. Achermann, *et al.*, "RoBoa: Construction and evaluation of a steerable vine robot for search and rescue applications," in *IEEE International Conference on Soft Robotics*, pp. 15–20, IEEE, 2021.

[11] J. D. Greer, L. H. Blumenschein, R. Alterovitz, E. W. Hawkes, and A. M. Okamura, "Robust navigation of a soft growing robot by exploiting contact with the environment," *International Journal of Robotics Research*, vol. 39, no. 14, pp. 1724–1738, 2020.

[12] M. Selvaggio, L. Ramirez, N. D. Naclerio, B. Siciliano, and E. W. Hawkes, "An obstacle-interaction planning method for navigation of actuated vine robots," in *IEEE International Conference on Robotics and Automation*, pp. 3227–3233, IEEE, 2020.

[13] D. A. Haggerty, N. D. Naclerio, and E. W. Hawkes, "Characterizing environmental interactions for soft growing robots," in *IEEE/RSJ International Conference on Intelligent Robots and Systems*, pp. 3335–3342, IEEE, 2019.

[14] "Robosoft 2023 competition." `https://robosoft2023.org/2023-competitions/`. Accessed: August 1, 2023.

[15] W. Fichter, *A theory for inflated thin-wall cylindrical beams*, vol. 3466. National Aeronautics and Space Administration, 1966.

[16] B. H. Do, V. Banashek, and A. M. Okamura, "Dynamically reconfigurable discrete distributed stiffness for inflated beam robots," in *IEEE International Conference on Robotics and Automation*, pp. 9050–9056, IEEE, 2020.

[17] B. H. Do, S. Wu, R. R. Zhao, and A. M. Okamura, "Stiffness change for reconfiguration of inflated beam robots," *arXiv preprint arXiv:2307.03247*, 2023.